

Silk fibroin hydrogel as mucosal vaccine carrier: induction of gastric CD4+TRM cells mediated by inflammatory response induces optimal immune protection against *Helicobacter felis*

Chupeng Hu^{a,b,*}, Wei Liu^{a,b,*}, Ningyin Xu^{a,b}, An Huang^{a,b}, Zhenxing Zhang^{a,b}, Menghui Fan^{a,b}, Guojing Ruan^{a,b}, Yue Wang^{a,b}, Tao Xi^{a,b} and Yingying Xing^{a,b}

^aSchool of Life Science and Technology, China Pharmaceutical University, Nanjing, People's Republic of China; ^bJiangsu Key Laboratory of Carcinogenesis and Intervention, China Pharmaceutical University, Nanjing, People's Republic of China

ABSTRACT

Tissue-resident memory T (T_{RM}) cells, located in the epithelium of most peripheral tissues, constitute the first-line defense against pathogen infections. Our previous study reported that gastric subserous layer (GSL) vaccination induced a "pool" of protective tissue-resident memory CD4+T (CD4+T_{RM}) cells in the gastric epithelium. However, the mechanistic details how CD4+T_{RM} cells form in the gastric epithelium are unknown. Here, our results suggested that the vaccine containing CCF in combination with Silk fibroin hydrogel (SF) broadened the distribution of gastric intraepithelial CD4+T_{RM} cells. It was revealed that the gastric intraepithelial T_{RM} cells were even more important than circulating memory T cells against infection by *Helicobacter felis*. It was also shown that gastric-infiltrating neutrophils were involved as indispensable mediators which secreted CXCL10 to chemoattract CXCR3+CD4+T cells into the gastric epithelium. Blocking of CXCR3 or neutrophils significantly decreased the number of gastric intraepithelial CD4+T_{RM} cells due to reduced recruitment of CD4+T cells. This study demonstrated the protective efficacy of gastric CD4+T_{RM} cells against *H. felis* infection, and highlighted the influence of neutrophils on gastric intraepithelial CD4+T_{RM} cells formation.

ARTICLE HISTORY Received 13 August 2020; Revised 21 September 2020; Accepted 26 September 2020



KEYWORDS Gastric intraepithelial CD4+T_{RM} cells; CXCR3; *Helicobacter felis*; silk fibroin hydrogel; neutrophils

Introduction

Tissue-resident memory T (T_{RM}) cells are critical mediators of immunity against infections in various tissues [1–6]. Typically, T_{RM} cells are located at barrier surfaces and, therefore, occupy the initial sites of infection and provide rapid protection. Clinical and preclinical trials have suggested that protection conferred by *Helicobacter pylori* (Hp) vaccines is largely dependent on engagement of differentiated CD4+T cells [7]. Although the protective effects of T_{RM} cells against infections have been described in the lung [2–4], vaginal mucosa [3], and skin [1]. Their roles in the gastric mucosa during infections have not been described thoroughly so far partially due to the rarity of native lymphocytes in stomach. In our previous study, mice immunized with alum-based *Helicobacter pylori* (Hp) vaccine through injecting into the gastric subserous layer (GSL) harbored a pool of Hp-specific CD4+T_{RM} cells in the gastric epithelium [8]. Hp infection occurs in the gastric epithelium where the intraepithelial CD4+T_{RM} cells are in a favourable

position to recognize the pathogen and initiate a protective response immediately [8]. However, the mechanistic details how CD4+T_{RM} cells form in the gastric epithelium are still unknown.

Migration of precursors of T_{RM} cells requires local inflammation or infection [9,10]. During acute of infection or inflammation, myeloid-lineage cells, including monocytes and neutrophils, infiltrate in local tissues and then secrete cytokines and chemokines, which induce entry of activated effector T cells into inflamed tissues [9]. Resident macrophages secrete CCL5 for CCR5+CD4+T cells, which sustain CD4+T_{RM} cells in the vaginal mucosa [11]. The local CXCL10 and CXCL9 have been shown to facilitate entry of CXCR3+CD8+T cells into the vaginal epithelium [12,13]. Interestingly, in the context of infection or immunization, epithelial cells are capable of acting as antigen-presenting cells by secreting cytokines and chemokines, and subsequently recruit circulating immune cells to initiate the local immune response [14–16]. In addition, the skin seems to enforce a constrained mode of migration of T cells,

CONTACT Yingying Xing  cpuskyxy@126.com  School of Life Science and Technology, China Pharmaceutical University, Nanjing 210009, People's Republic of China; Jiangsu Key Laboratory of Carcinogenesis and Intervention, China Pharmaceutical University, Nanjing 210009, People's Republic of China *These authors contributed equally to this work.

 Supplemental data for this article can be accessed at <https://doi.org/10.1080/22221751.2020.1830719>

© 2020 The Author(s). Published by Informa UK Limited, trading as Taylor & Francis Group, on behalf of Shanghai Shangyixun Cultural Communication Co., Ltd This is an Open Access article distributed under the terms of the Creative Commons Attribution-NonCommercial License (<http://creativecommons.org/licenses/by-nc/4.0/>), which permits unrestricted non-commercial use, distribution, and reproduction in any medium, provided the original work is properly cited.

which also induces formation of T_{RM} cells [13,17]. Taken together, it might be expected that myeloid-lineage cells, gastric epithelial cells, or the epithelial environment may aid entry of CD4⁺T cells into the gastric epithelium. In this study, we focused on the relationship between vaccine-induced inflammatory response and induction of gastric CD4⁺ T_{RM} cells, and explored the protective efficacy of gastric CD4⁺ T_{RM} cells against *H. felis* infection.

Methods

Ethics approval and consent to participate

All animal experiments were performed with the approval of Ethic Committee for Animal Experimentation of China Pharmaceutical University (202009007).

Animals

Female 6-8-week-old C57BL/6 mice, transgenic EGFP mice (C57BL/CAG-EGFP) and transgenic CD45.1 mice (congenic C57BL/6) were obtained from the Comparative Medicine Center of Yangzhou University, Model Animal Research Center of Nanjing University and Model Organisms Animal Research Center of Shanghai, respectively. They were bred in the Animal Experimental Center of China Pharmaceutical University.

Vaccine preparation

Purified CTB-UE-CF (CCF) protein was constructed by cholera toxin B, multi-epitopes from *H. pylori* urease, and self-adjuvant regions from *S. typhimurium* phase I flagellin FliC, and the preparation of CCF was undertaken as described previously [19]. Briefly, CCF protein was expressed by *Escherichia coli* Rosetta (DE3) cells with pET-28a-CCF. First, the protein was purified using nickel-affinity chromatography (GE Healthcare, Amersham, UK), followed by anion-exchange chromatography with DEAE Sepharose FF (Amersham Pharmacia Biotech Uppsala, Sweden). Alum-based vaccine (Al+CCF) was prepared with an equal volume of CCF solution and alum adjuvant. A silk fibroin hydrogel-based vaccine (SF+CCF) was prepared: CCF solution was mixed with silk fibroin protein, and then mixed with an equal volume of 90% polyethylene glycol-400. The final concentration of CCF and silk fibroin protein was 1.5 and 40 mg/mL, respectively. Per mouse was injected with 10.5 µg/mouse.

Gastric subserous layer (GSL) vaccination

C57BL/6 mice were anesthetized (50 mg/kg pentobarbital sodium, i.p.). Mice were placed on a thermostatic hot plate under aseptic conditions. After shaving off the right side of the abdomen, a 1 cm-wide skin incision was made above the stomach. Subsequently, the stomach was exposed using forceps. The GSL of the greater curvature was injected with 7 µL of vaccine (CCF+SF or CCF+Al) using a micro-syringe with a 33 G needle. Next, the peritoneal incision was uninterruptedly sutured uninterruptedly with a 7-0 polyglycolic acid (PGA) absorbable suture. Then, the skin incision was done using interrupted sutures (Shanghai Pudong Jinhuan Medical Products, Shanghai, China.).

Parabiosis mice

8-week-age CD45.1 and CD45.2 mice were co-housed for 2 weeks before surgery. Those mice were anesthetized (50mg/kg pentobarbital sodium, i.p.), wiped with iodine in the hair-removal area, and placed on a thermostatic hot plate under aseptic conditions. After shaving the corresponding lateral aspects of each mouse, a matching incision was made on the lateral skin from the elbow to the hip. Then, and the tibia and ulna of each mouse were bound together with a 3-0 PGA non-absorbable suture to join the forelimbs and hindlimbs together. A matching skin incision of each mouse was sutured together using a 4-0 PGA absorbable suture (Shanghai Pudong Jinhuan Medical Products).

Preparation of single-cell suspensions from gastric tissue

Single-cell suspensions were prepared as described [8]. In brief, the entire stomach of mice was placed into 15 mL of RPMI 1640 buffer containing 10 mM HEPES, 10% phosphate-buffered saline (PBS), 4 mM ethylenediamine tetraacetic acid (EDTA), and 0.5 mM dithiothreitol (DTT). Gastric epithelial leukocytes (GELs) were isolated by agitation at 250 rpm for 30 min at 37°C. Then, gastric remaining leukocytes (GRLs) were isolated. Briefly, after isolating GELs, the stomach was minced. Then, the content was placed into 15 mL of RPMI 1640 buffer containing 10 mM HEPES, 10% PBS, 4 mM EDTA, and 0.5 mM dithiothreitol. GRLs were isolated by shaking at 250 rpm for 20 min at 37°C. A single-cell suspension was obtained by passing it through a 70-µm cell strainer. The leukocytes suspension was purified with a 67%/44% Percoll™ gradient. FACS assay showed that most stomach leukocytes are viable after their isolation (Figure S2C).

Preparation of single-cell suspensions from blood and lymphoid organs

Single-cell suspensions from the spleen (SP) and mesenteric lymph nodes (MLN) were obtained by gentle pushing through a 70- μ m cell strainer. Then, blood and spleen tissue were incubated with 5 mL of erythrocyte lysis buffer and washed twice with 10 mL of PBS containing 5% FBS. Then, cells were collected for FACS analyses.

Analyses of antigen-specific CD4+T cells

Antigen-specific CD4+T cells were prepared as described previously [8]. In brief, to detect antigen-specific CD4+ T cells, naive splenocytes were labelled by using CFSE. After being pulsed by antigen CCF (150 μ g/mL), the splenocytes were activated as APC and then used to stimulated gastric lymphocytes for 12 h in RPMI 1640 buffer containing 10% fetal bovine serum and brefeldin A (5 μ g/mL). After collection, the cells were stained for interferon (IFN)- γ and interleukin (IL)-17 to detect antigen-specific CD4+T cells.

FACS analyses and sorting

Purified single-cell suspensions from blood, lymphoid organs and gastric tissue were stained with the following antibodies: anti-CD45 (30-F11), anti-CD45.1 (A20), anti-CD45.2 (104), anti-IFN- γ (XMG1.2), anti-IL-17A (TC11-18H10.1), anti-F4/80 (BM8), anti-Ly6G (1A8), anti-CD3 (145-2C11), anti-CD90.2 (30-H12), anti-CD4 (GK1.5), anti-CD11b (M1/70), anti-CD8 α (53-6.7), anti-CD19 (6D5), anti-major histocompatibility (MHC) class II (M5/114.15.2), anti-Ly6C (HK1.4), anti-Gr-1 (RB6-8C5), anti-CCR1 (6588-5), anti-CCR3 (5E8), anti-CCR5 (HM-CCR5), anti-CCR7 (4B12), anti-CXC3R (CXCR3-173), anti-CD326 (C068C2) and anti-CD11c (N418). Samples were incubated for 20 min on ice in the dark. Multi-parameter analyses were undertaken on a BD FACSTM Aria II.

The FACS sorting of gastric epithelial cells, monocytes, and neutrophils

Purified single-cell suspensions from gastric epithelium and blood were prepared as described above. The samples from gastric epithelium were stained with antibodies against anti-CD45 (catalog number, 30-F11), anti-CD11b (M1/70), anti-Ly6C (HK1.4), anti-Gr-1 (RB6-8C5) and anti-CD326 (C068C2). The samples from blood were stained with antibodies against anti-CD45 (catalog number, 30-F11), anti-CD11b (M1/70), anti-Ly6C (HK1.4), anti-Gr-1 (RB6-8C5). Cell sorting was done on BD FACS Aria II SORP (Becton Dickinson). Monocytes

gate on CD45+CD11b+Gr1+Ly6C+, neutrophils gate on CD45+CD11b+Gr1+Ly6C^{int}. gastric epithelial cells gate on CD45-CD11b-CD326+.

Immunofluorescent staining

Frozen sections of gastric tissue (20 or 10 μ m) were cut and dried at room temperature. After blockade in a 5% bovine serum albumin PBS solution for 1 h, sections were stained with an Alexa Fluor[®] 488-anti-CD4 (GK1.5; Biolegend) antibody and/or purified anti-CD11b (M1/70, Biolegend) followed by goat anti-rat immunoglobulin (Ig)G2a/IgG2b Alexa Fluor 488/594 antibody (Biolegend). Slides were washed, counterstained with DAPI to visualize cell nuclei and analysed by fluorescence microscopy. All images were acquired with a Panoramic 250 Flash III Scanner (3D Histech, Budapest, Hungary).

Quantitative RT-PCR

RNA was extracted from gastric epithelial cells, monocytes, and neutrophils using TRIzol[®] Reagent (Invitrogen, Carlsbad, CA, USA), and reverse transcribed into cDNA using moloney murine leukemia virus reverse transcriptase (Promega, Fitchburg, WI, USA) as described previously [20]. RT-qPCR was done using conventional SYBR green-based quantification method. Primers (forward and reverse, respectively) were designed by GENEWIZ based on the follows: GAGCTGAACGGGAAGCTCAC and AGTC-TAGCCCAAGATGCCCT for GAPDH; GGAG-TATTTCTACACCAGCAGCAA and CACACACTTGGCGGTTTCCT for CCL5; AAT-CATCCCTGCGAGCCTATC and TCAGA-CATCTCTGCTCATCATTCTT for CXCL10.

FTY720 treatment

Mice were administered FTY720 (1 mg/kg, i.p.) daily to blockade egress of circulating memory T cell from a secondary lymphoid organ.

Blocking antibodies experiments in vivo

Before being challenged with *Helicobacter felis*, the mice were treated with anti-Gr-1 antibody or Isotype Rat IgG2b (250 μ g, i.p.) daily for 3 days to deplete inflammatory neutrophils and monocytes. For inhibition of migration of CD4+T cells, mice were injected (i.p.) twice with a dose of 200 μ g of anti-CXCR3 (clone:CD183) or Armenian Hamster IgG and anti-Ly6G (clone:1A8) or Rat IgG2a 7 days before immunization with the vaccine. Depletion *in vivo* was confirmed through FACS analyses of the cell suspension from blood.

Culture and transfer of EGFP+CD4+T cells

For priming of effector EGFP+CD4+ T cells *in vitro* [21], EGFP+CD4+T cells from the splenocytes of EGFP mice were sorted. For skewing to a Th1 phenotype, IL-12 (10 ng/mL), and anti-IL-4 (40 mg/mL; 11B11) were added to the culture. For skewing to a Th17 phenotype, IL-6 (50 ng/mL), transforming growth factor (TGF)- β (1ng/ml), IL-23 (5 ng/mL), anti-mouse IL-4 (10 μ g/mL), and anti-mouse IFN- γ (10 μ g/mL) were added to the culture. Briefly, at day 0, coat of plastic petri with anti-mouse CD3 and incubate at 37°C for 2 h. CD4+T cells (10^6 /mL/well) were cultured in the presence of relevant antibodies/cytokines. Fresh medium with the same concentration of antibodies/cytokines was added to cells at day 3, and collected at day 6 of culture. Effector EGFP+CD4+T cells (10^5 to 0.5×10^6) were enriched using magnetic beads and subsequently injected into the GSL of wild-type mice. For pertussis toxin (PTX) treatment, the activated EGFP+CD4+T cells were treated for 90 min *in vitro* with PTX (100 ng/mL).

Culture of infection with *H. felis*

The CCF protein contains multi-epitopes from the *H. pylori* urease which is same to *H. felis* urease. Because *H. felis* is more suitable for immunization research [22,23], our study used *H. felis* strain. *H. felis* strain (ATCC 49179) was cultured on an inter-layer of solid and liquid medium added with 7% heat-inactivated fetal bovine serum and vancomycin (10 μ g/mL) under microaerophilic conditions at 37°C. At 3–4 days after culture, *H. felis* were harvested through centrifugation and re-suspended in fresh medium. All the mice were challenged (p.o.) with 0.5×10^9 *H. felis* in 200 μ L of medium once. After 3 days, tissues from these mice were harvested and analysed.

Colonization of *H. felis* in gastric tissue

To detect colonization of *H. felis* in gastric tissue, RT-qPCR was done to detect *H. felis*-16S expression in gastric tissue. The total DNA of gastric tissue was extracted with a TIANamp Genomic DNA kit according to the manufacturer (Tiangen Biotech, Beijing, China) instructions. Quantitation was done using the ChamQ™ Universal SYBR qPCR master mix (Thermo Fisher, Boston, MA, USA). Primers (forward and reverse, respectively) were designed by GENEWIZ based on the follows: GAGCTGAACGG-GAAGCTCAC and AGTCTAGCCCAAGATGCCCT for GAPDH; TTCGATTGGTCCTACAGGCTCAGA and TTCTTGTGATGACATTGACCAACGCA for *H. felis*-flaB. Analysis and fold-change were determined using the CT method.

Statistical analyses

Data are the mean \pm SD. Statistical analyses were carried out using ANOVA or the Student's *t*-test with the GraphPad Prism 6.0, $P < 0.05$ was considered significant.

Results

SF as a vaccine carrier not only reduced stomach damage but also induced broad distribution of CD4+T cells in the gastric mucosa

To avoid stomach damage from alum adjuvant [8], we utilized SF, a biocompatible and biodegradable biomaterial, as a vaccine carrier. Laparotomy was carried out on C57BL/6 mice to access the stomach, and SF+CCF or Al+CCF was injected into the GSL (the definition of CCF refers to methods section). 180 days after immunization, compared with the SF+CCF group, Al+CCF group suffered from gastric granulation as evidenced by histological staining (as indicated by the arrows in Figure S1A and Figure S1B), indicating persistent damage to gastric tissue.

To investigate if the SF-based vaccine increased the immune response, we injected SF+CCF or Al+CCF into the GSL of mice. At 7 days after immunization, immunolocalization assays showed more pronounced CD4+T cells infiltration into the gastric mucosa not only near the vaccination site but also in distant epithelial tissues in the SF+CCF group compared with that in the Al+CCF group (Figure 1(A and B)), suggesting that SF+CCF formulation induced wider distribution of CD4+T cells in the gastric mucosa. Staining of intracellular cytokines showed that both vaccine formulations induced production of antigen-specific CD4+T cells. However, inclusion of SF in the vaccine formulation resulted in a significantly higher number of antigen-specific, IFN- γ /IL-17A-producing CD4+T cells (Figure 1(C and D)). To be noted, only SF did not induce Ag-specific, IFN- γ /IL-17A-producing CD4+T cells in gastric tissue (Figure S2A and B). Most infiltrating CD4+T cells located close to the epithelium 28 days after immunization, albeit the density of CD4+T cells in mucosa decayed. Notably, at this time point, most CD4+T cells were located close to the epithelium, which was confirmed by the distinct epithelial architecture of stomach (Figure S3B). it was tempting to speculate that broader distribution of CD4+T_{RM} cells emerged in gastric epithelial region mice in the SF+CCF group compared with that in the Al+CCF group (Figure S3A). Compared with Al+CCF group, the SF+CCF group had more antigen-specific, IFN- γ /IL-17A-producing CD4+T cells (Figure S3C, D) occupying larger area of epithelium. Overall, inclusion of SF in the vaccine formulation induced a pronounced immune response and wider distribution of CD4+T cells in the gastric mucosa under acute or steady-state conditions.

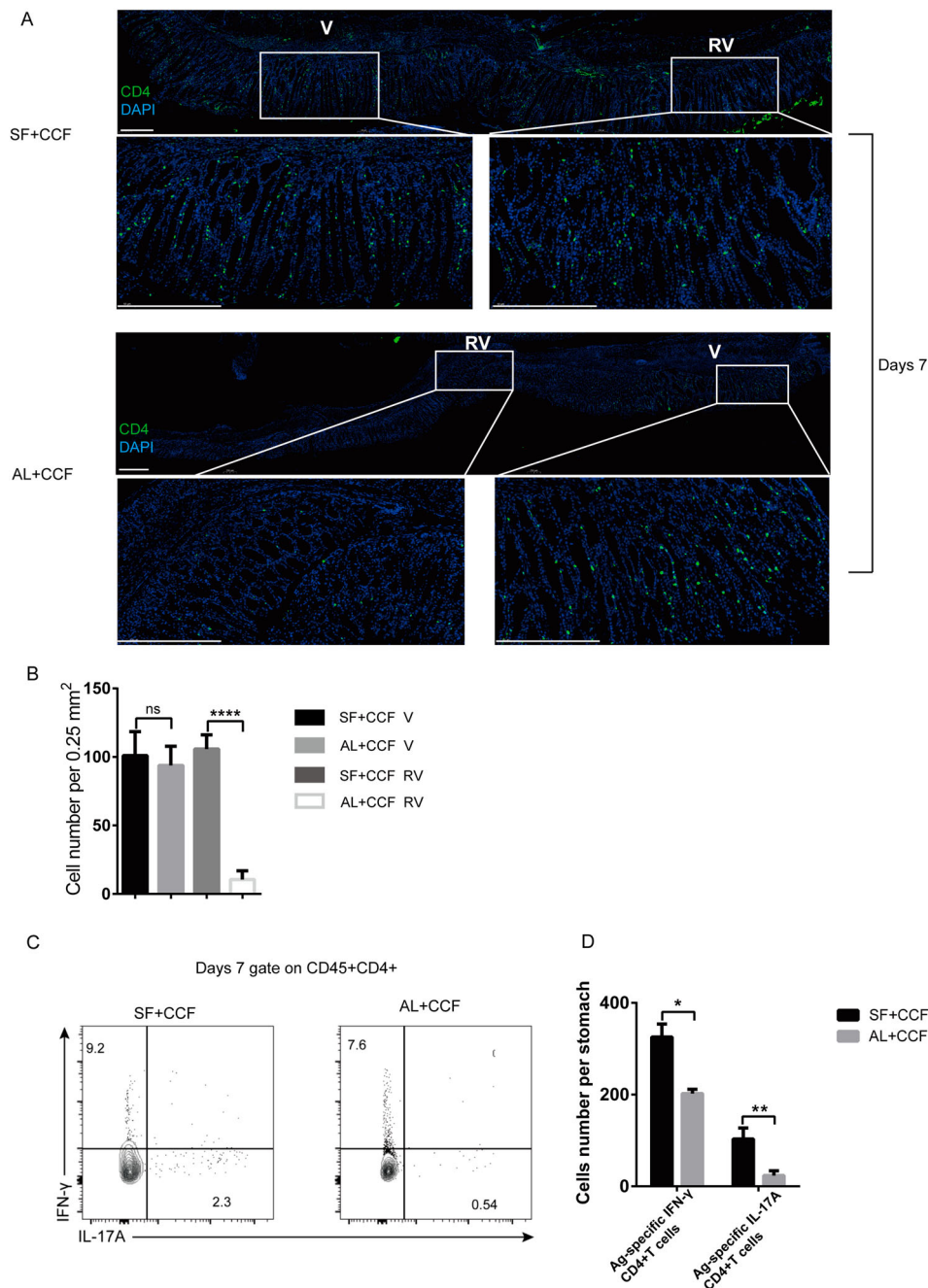


Figure 1. Vaccine-induced infiltration of CD4+T cells into gastric tissue. Mice were immunized with SF+CCF or AI+CCF by GSL vaccination. Briefly, a laparotomy was done to expose the stomach, and 7 μ L of a vaccine formulation was injected into the subserosa layer of the stomach. Incisions in the peritoneum and skin were sutured (SF+CCF, silk fibroin hydrogel-based vaccine; AI+CCF, alum adjuvant-based vaccine; GSL, gastric subserous layer). At 7 days after immunization, mice were sacrificed, and gastric tissue was collected for further testing. (A) Frozen sections of gastric tissue from immunized mice were stained with antibodies against CD4, nuclei are depicted by DAPI staining; scale bar = 100 μ m (n=5 mice per group). (B) Counts of CD4 cells in area of the V or RV per 0.25 mm² were randomly chosen and calculated (green, CD4; blue, DAPI; V, vaccination site; RV, remote area of vaccination site). (B and C) Antigen-specific CD4+T cells in the stomach were counted by staining of intracellular cytokines. Single-cell suspensions from gastric tissue were stimulated with 10⁶ naïve CFSE-labeled splenocytes preloaded with antigen CCF, and then the percentage and number of IFN- γ /IL-17-producing CD4+T cells was calculated. Values are the mean \pm SD (n=5 mice per group). Data are representative of two independent experiments. *P*-values were obtained using the Student's *t*-test. **P* < 0.05.

CD69+CD4+T_{RM} cells stayed in the gastric epithelium long-term without recirculating

Next, to determine the phenotype of gastric intraepithelial CD4+TRM cells, we analysed the gastric intraepithelial CD4+TRM cells, 7, 21, 28, 56 and 168 days after GSL vaccination by flow cytometry. It was

found that infiltrating CD4+TRM cells expressed CD69 and moderate CD103 compared with circulating CD4+T cells (Figure 2(C)). CD4+T cells from the gastric epithelium expressed CD44 but not CD62L (Figure 2(D)). CD4+T cells exhibited highest expression of CD69 28 days post-immunization (Figure 2(A and B)). Strikingly, most gastric

intraepithelial CD4+T cells showed high expression of CXCR3 and CCR5 but not CCR1, CCR3 or CCR7 (Figure 2(E)).

To further distinguish the selective ability of local immunization to confer protective immunity, we used CD45.1 and CD45.2 parabiosis models. Full chimerism was achieved in the systemic circulation within 3 weeks of parabiosis (Figure S4 A-C). Gastric intraepithelial CD4+T_{RM} cells were analysed 49 days after immunization. Host-derived CD4+T_{RM} cells were distributed mainly within the gastric epithelium, whereas few donor-derived circulating CD4+T cells were found at the periphery of the gastric epithelium (Figure 2(F and G)). Collectively, these results demonstrated that GSL vaccination induced generation of CD69+CD4+T_{RM} cells which constitute a gastric intraepithelial-resident population which did not recirculate.

Vaccine-induced CD4+T_{RM} cells conferred optimal protection against *H. felis* insult

We then investigated if the GSL-vaccination model in mice provided persistent protection against *H. felis* insult, mice were challenged with *H. felis* 4 and 12 months after the single-dose immunization. As expected, substantial reduction of bacterial colonization was found in vaccinated mice compared with that in naïve mice (Figure S5A, B). To further distinguish the role of tissue-resident T cells from circulating T cells, immunized mice were treated with FTY720 to block lymphocyte egress from lymph nodes [11] before being challenged with *H. felis*. T_{RM} cells contributed to a reduction of colonization of *H. felis* in early protection (Figure 3(A and B)). Additionally, compared with group 3, the number of monocytes and neutrophils was increased substantially in the gastric epithelium of groups 1 and 2 (Figure 3(C and D)). Depletion of monocytes and neutrophils resulted in an increased number of gastric *H. felis*, suggesting that early protection was enhanced by monocytes and neutrophils (Figure 3 (E and F)).

Next, we compared the ability of tissue-resident lymphocytes versus circulating memory lymphocytes to mediate protection against a *H. felis* challenge using various parabiotic combinations. Mice only relying on circulating memory cells (group 2) showed impaired ability to suppress colonization of *H. felis* compared with the fully protected mice in group 3 and 4 that harboured functional T_{RM} cells (Figure 3 (G and H)). Taken together, these data demonstrated that the GSL vaccination that induced generation of T_{RM} cells conferred optimal protection against *H. felis* insult, and that early protection was enhanced by monocytes and neutrophils.

CD4+T_{RM} cells mainly distributed in the epithelium of the stomach

We determined if CD4+T cells tended to disperse in the gastric epithelium. Along with the injection of SF-based vaccine into the GSL, *in vitro*-activated EGFP+CD4+T cells containing 50% Th1 cells and 50% Th17 cells were also injected into the GSL to examine if EGFP+CD4+T cells could develop into epithelium-lodged CD69+ T_{RM} cells. At day 7, the injected fluorescent cells were observed in the gastric epithelium (Figure 4(A)), and most EGFP+CD4+T cells eventually translocated to the gastric epithelium by day 28 (Figure 4(B)). Furthermore, to show that entry into the epithelium was necessary for the formation of T_{RM} cells, we treated the *in vitro*-differentiated EGFP+CD4+ T cells with PTX before injecting (Figure 4(C) and Figure S10). While untreated cells migrated into the epithelium and became a population of CD69+EGFP+CD4+T_{RM} cells after GSL injection, PTX treatment blocked infiltration of EGFP+CD4+T cells to the epithelium and expression of CD69 *in vivo* (Figure 4(D and E)). Additionally, at day7 and 28 post injection of EGFP+CD4+T cells, Most of EGFP+CD4+T cells with higher expression of CXCR3 were distributed in the gastric epithelium (Figure 4(F)). Interestingly, compared with the population of CD4+CD69-T cells, substantially higher expression of CXCR3 was observed in the population of CD4+CD69+T cells (Figure 4(G and H)). Taken together, these data suggested CXCR3+CD69+CD4+T_{RM} cells tended to be disperse in the gastric epithelium.

Inflammatory Gr-1+cells induced by GSL vaccination contributed to mediation of formation of CD4+T_{RM} cells in the gastric epithelium

We injected CCF+SF or CCF+PBS into the GSL of mice. At days 0, 1, 3, and 7, subsets of immune cells from the stomach of these mice were isolated and analysed (Figure 5(A and C)). The population of monocytes and neutrophils migrated rapidly into the stomach and arrived, peaked and became apoptotic at days 1, 3 and 7, respectively (Figure 5(B), Figure S6A, B). While the number of CD4+T cells peaked at day 7, they became apoptotic at day 14 (Figure 5 (D), Figure S6C). CD11b+cells and CD4+T cells were colocalized in the gastric mucosa at day 3 (Figure 5(G)). The population of monocytes and neutrophils was highest frequency in the gastric mucosa (Figure 5(E, F and H)). Hence, we examined whether Gr-1+ cells were involved in gastric CD4+T_{RM} cells formation by treating mice with Gr-1 blocking antibody. Antibody-treated mice showed remarkable reduced gastric intraepithelial CD69+CD4+T_{RM} and the total number of total CD4 T_{RM} compared with

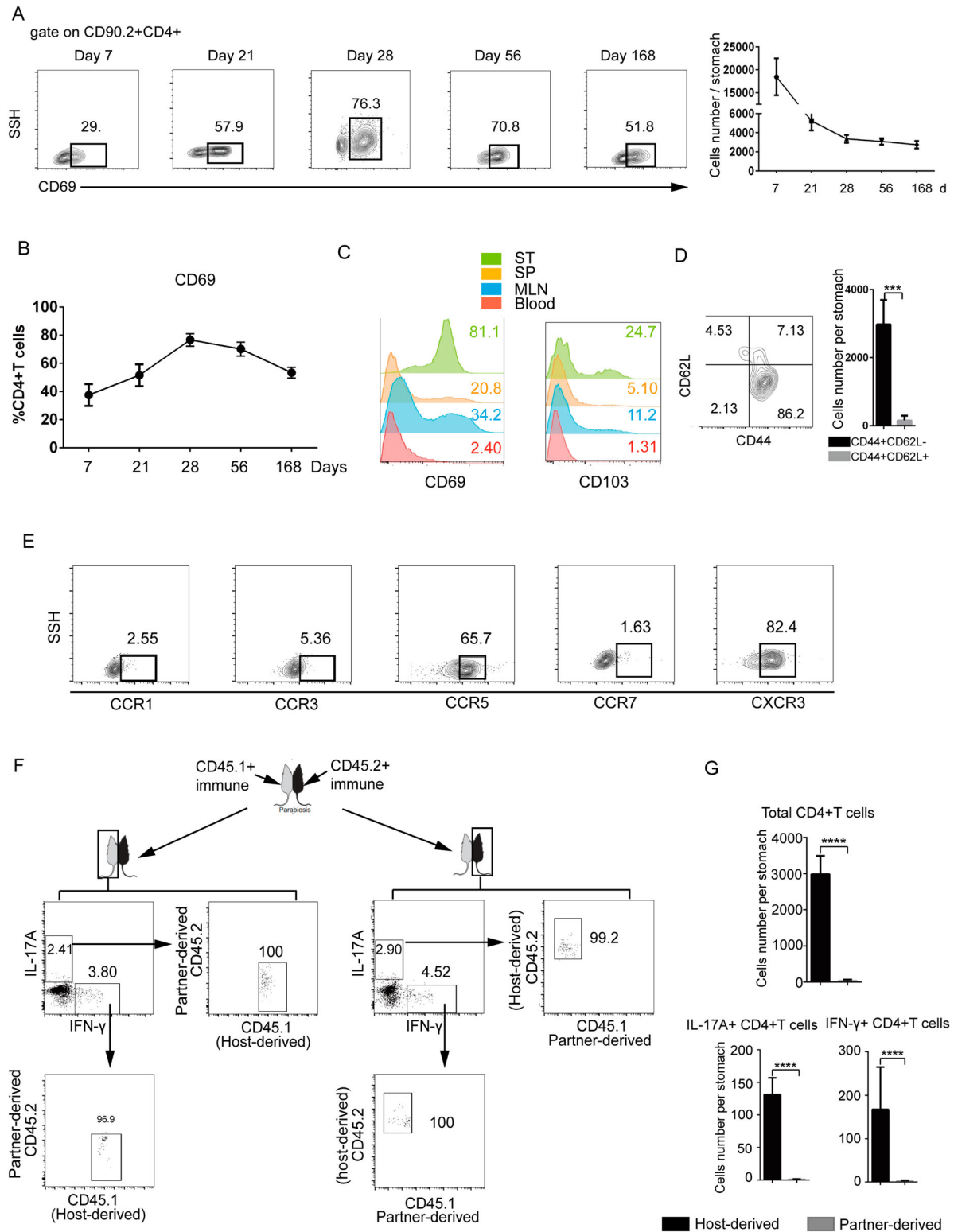


Figure 2. Characterization of gastric intraepithelial CD4+TRM cells. Mice were immunized with SF+CCF by GSL vaccination, as described in Figure 1. (A and B) At 7, 21, 28, 56 and 168 days after immunization, CD69 expression of gastric intraepithelial CD4+T cells was analysed by flow cytometry. (C) At 28 days after immunization, expression of CD69 and CD103 of CD4+T cells from the gastric epithelium (ST), spleen (SP), blood, and mesenteric lymph nodes (MLNs) was measured. (D and E) At 28 days after immunization, expression of CD62L, CD44, CCR1, CCR3, CCR5, CCR7 and CXCR3 of gastric intraepithelial CD4+T cells was measured. (F and G) CD45.1+ and CD45.2+ mice immunized with SF+CCF 28 days previously underwent parabiotic surgery. At 21 days after parabiosis, the population of total, antigen-specific host, and donor-derived CD4+T cells in the gastric tissues of parabiotic mice was analysed by flow cytometry. Values are the mean \pm SD (4–5 pairs). *P*-values were obtained using the Student's *t*-test. Data are representative of two independent experiments. *****P* < 0.0001.

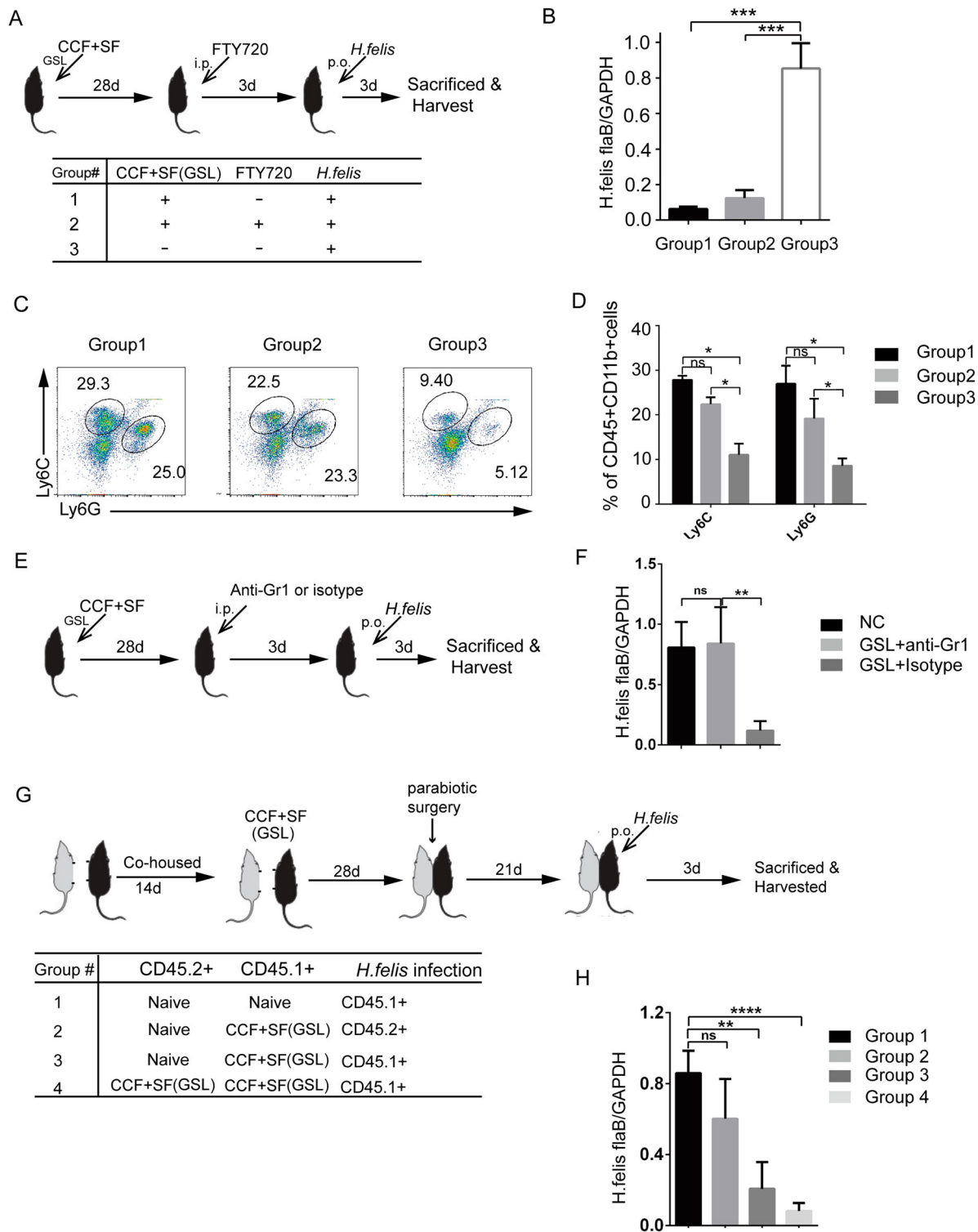


Figure 3. Vaccine-induced TRM cells are superior to circulating T cells for mediating protection against *H. felis* insult. Mice were immunized with SF+CCF by GSL vaccination, as described in Figure 1. (A–D) 28 days later, mice were injected (i.p.) with FTY720 (1 mg/mL) or PBS daily for 3 days as indicated in the table. Then, mice were challenged with *H. felis*. 3 days later, colonization of the stomach by pro-inflammatory neutrophils and monocytes was analysed. (E and F) At 28 days after immunization, mice were injected (i.p.) with anti-Gr-1 antibody or Isotype Rat IgG2b (200 µg) daily for 3 days. Then, mice were challenged with *H. felis*. 3 days later, colonization of the stomach was analysed. (G and H) According to the table, the indicated CD45.1+ and CD45.2+ mice, naive or immunized with SF+CCF 28 days previously, underwent parabiotic surgery. At 21 days after parabiosis, the indicated partner was challenged with *H. felis*. 3 days later, colonization of the stomach of indicated mice was detected. Values are the mean \pm SD ($n = 4-5$). Data are representative of two independent experiments. P -values were obtained using ANOVA. * $P < 0.05$, ** $P < 0.01$, **** $P < 0.0001$, n.s., not significant.

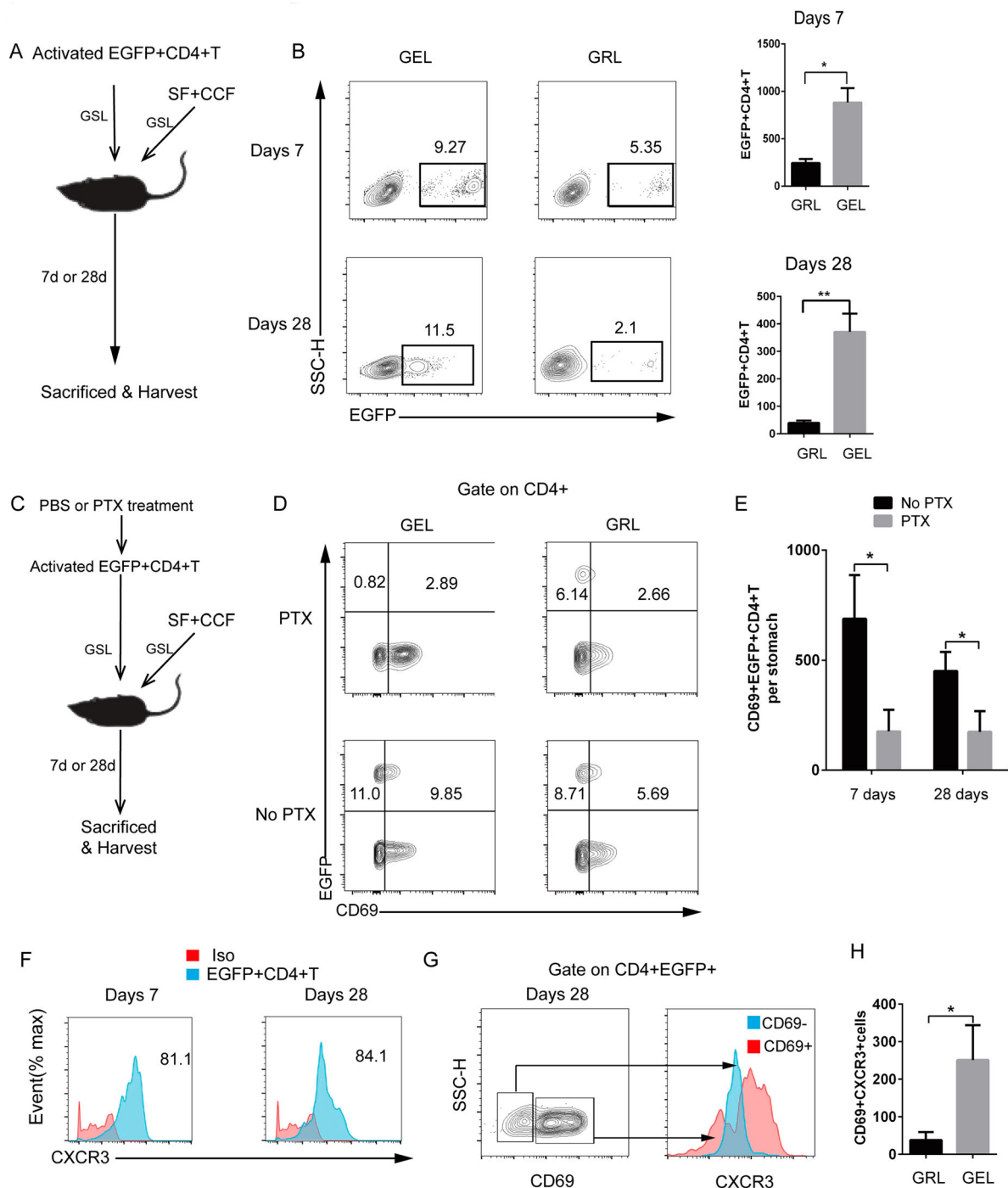


Figure 4. Differentiated EGFP+CD4+TRM cells formed in the gastric epithelium. (A) In vitro-activated EGFP+CD4+T cells were injected into the GSL of wild-type naive mice immunized with SF+CCF by GSL simultaneously. Mice were sacrificed 7 and 28 days after transfer. (B) EGFP+CD4+T cells from the GELs and GRLs of mice were analysed using flow cytometry (GELs, gastric epithelial leukocytes; GRLs, gastric remaining leukocytes). (C) In vitro-activated EGFP+CD4+T cells before being injected into GSLs of wild-type naive mice were treated with pertussis toxin (PTX) or PBS (no PTX). (D) At 7 and 28 days after transfer, expression of EGFP and CD69 in CD4+ cells was analysed. (E) Then, CD69+EGFP+CD4+T cells were quantified. (F) At 7 and 28 days after transfer of EGFP+CD4+T cells, CXCR3 expression in EGFP+CD4+T cells from GELs was measured. (G) At 28 days after transfer, CXCR3 expression of EGFP+CD4+CD69⁻ cells and EGFP+CD4+CD69⁺ cells from GELs was measured. (H) Then, quantification of CXCR3+CD69+EGFP+CD4+T cells from GELs and GRLs was done. Values are the mean \pm SD ($n = 5$). Data are representative of two or three independent experiments. P -values were obtained using ANOVA. * $P < 0.05$, ** $P < 0.01$.

untreated mice (Figure 5(I–K)), whereas Gr-1 antibody treatment did not impair the percentage of CD4+T cells of spleen (Figure S7). Overall, vaccine-induced Gr-1+ cells were associated with formation of gastric intraepithelial CD69+CD4+T_{RM} cells.

CXCL10-producing neutrophils were involved in gastric epithelial entry of vaccine-induced CD4+T cells

Next, we sought to identify the mechanistic details how Gr-1+ cells are associated with CD4+T_{RM} cells

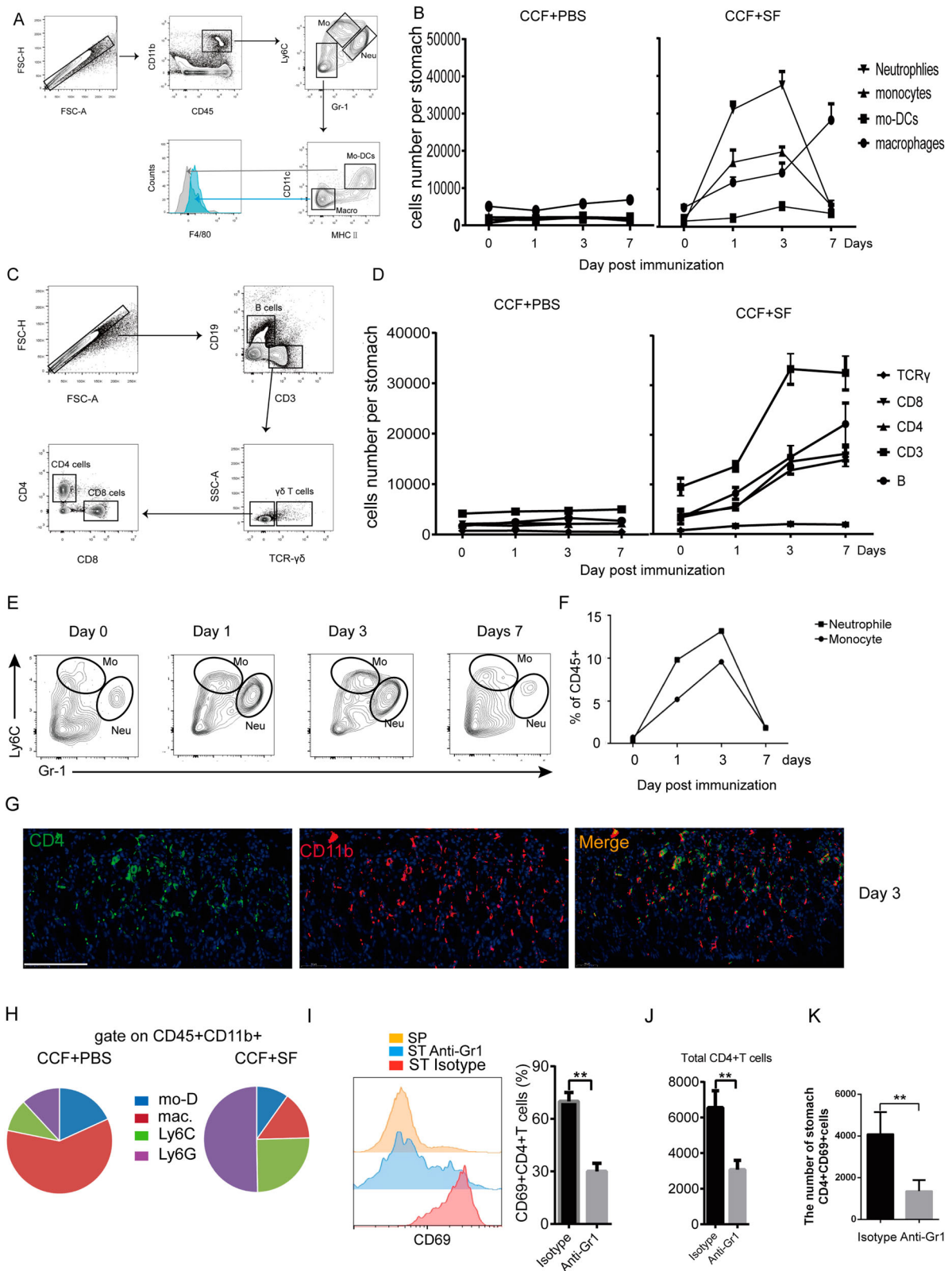


Figure 5. Inflammatory neutrophils and monocytes were associated with the location of gastric intraepithelial CD4+TRM cells. Mice were immunized with CCF+SF or CCF+PBS by GSL vaccination, as described in Figure 1. Myeloid-lineage cells and lymphocytes were gated according to (A) and (C), respectively. (B and D) These graphs illustrate the total numbers of several immune-cell subsets in the gastric mucosa. (E and F) The proportion of neutrophils and monocyte was counted using flow cytometry. (G) At 3 days after immunization, frozen sections of gastric tissue from immunized mice were stained with antibodies against CD4 (green) and CD11b (red), and nuclei are depicted by DAPI (blue); scale bar = 100 μm. (H) At 3 days after immunization, the total CD11b+ population from the gastric epithelium was analysed. (I, J and K) Mice were treated with anti-Gr1 antibody or Isotype daily. Three days later, mice were immunized with CCF+SF by the GSL. At 28 days after immunization, the population of gastric intraepithelial CD69+CD4+T cells was analysed using flow cytometry (SP, spleen; ST anti-Gr1, the stomach of anti-Gr1-treated mice; ST Isotype (Rat IgG2b), the stomach of Isotype-treated mice). Values are the mean ± SD (n = 5). Data are representative of two independent experiments. *P*-values were obtained using t-test. ****P* < 0.001, n.s., not significant.

formation in the gastric epithelium. Previously, we showed high expression of CCL5, CXCL10 but not CXCL9 in gastric tissue at day 2 post GSL vaccination (8). High expression of CXCR3 and CCR5 in gastric intraepithelial CD4⁺ T cells was noticed (Figure 2 (E)). Hence, we measured expression of CCL5 and CXCL10 in epithelial cells, monocytes and neutrophils.

Neutrophils, epithelial cells, and monocytes were sorted for qPCR analyses at day 3 post-immunization (Figure S8). The results suggested that neutrophils showed higher-level expression of CXCL10 compared with epithelial cells and monocytes (Figure 6(A)). To examine if gastric epithelial entry of CD4⁺T cells was linked to neutrophils in a CXCR3 pathway, we treated GSL-vaccinated mice with Ly6G antibody and CXCR3 antibody. As expected, 7 days after immunization, antibody-treated mice showed a significant reduction in the number of gastric intraepithelial CD4⁺T cells compared with that in isotype-treated mice (Figure 6(B–D)), whereas Gr-1 antibody treatment did not impair the percentage of CD4⁺T cells of spleen (Figure S9). Additionally, 28 days after immunization, blocking CXCR3 or neutrophils resulted in generation of significantly fewer CD69⁺CD4⁺T_{RM} cells compared with untreated mice (Figure 6(E and F)), suggesting that neutrophils facilitated the entry of CXCR3⁺CD4⁺T cells into the gastric epithelium and formation of CD69⁺ CD4⁺T_{RM} cells.

Discussion

Growing evidence emphasizes the importance of memory T cells (T_{RM}) located in peripheral tissues against various infections and to maintain long-term immune surveillance, including detection of infected cells and responding rapidly even before recruitment of circulating memory T cells (21). Deciphering mechanisms of migration, formation, maintenance and recall response of T_{RM} cells are essential to understand of host–pathogen interactions and also instructive for vaccine development.

During the acute stage of infection or immunization, various effector T cells migrate into inflamed tissues. Subsequently, heterogeneous populations of effector T cells differentiate into memory T cells as a result of differential expression of transcription factors, cytokine receptors and other cell-surface molecules [9]. These molecular signals contribute to formation and survival of T_{RM} cells. For instance, TGF- β - induced signals to regulate T-bet expression in CD8⁺T_{RM} cells, which mediates formation of T_{RM} cells and CD103 expression [4]. Indeed, migration of effector T cells into peripheral tissues is important for subsequent formation of T_{RM} cells [24]. The mammalian target of rapamycin (mTOR) pathway may

participate in this process by facilitating migration of effector T cells into mucosal tissues [25]. In lung, CXCR3 is required for appropriate localization of effector T cells to the epithelium, and CXCR6 directs entry of CD8 T_{RM} cells into the airways [26]. In addition, “tissue-homing” pattern is important factor for formation of T_{RM} cells. For example, skin-homing T cells express CCR4 and/or CCR10, which interact with the dermal-associated CCL17 and CCL27, respectively [27,28]. In comparison, gut-homing T cells express α 4 β 7-integrin, which binds to Madcam-1 [29], and CCR9, which interacts with gut-associated CCL25 [30]. Our current work showed that a coordinated Gr-1⁺cells infiltration of the stomach enforced a constrained mode of migration of T cells, which also contributed to formation of the gastric intraepithelial T_{RM} cells. Also, our data showed that gastric infiltration of neutrophils attracted CXCR3⁺CD4⁺T cells through CXCL10 secretion, in consistence with previous studies showing that formation of T_{RM} cells is required for the inflammatory response [9,10]. Our published finding showed that CXCL10 but not CXCL9 were at high level in the gastric tissue at day 2 post GSL vaccination [8]. A high proportion of CD69⁺CD4⁺T_{RM} cells expressed CXCR3 in the gastric epithelium, which is also the case for lung-resident CD4⁺T_{RM} cells [4,31]. CXCR3 expression contributes to the entry of CD8⁺T_{RM} cells in the skin epidermis [13]. Indeed, CXCR3 has been shown to be involved in localization of CD8 T cells to infected areas in non-lymphoid tissue, including the brain, lung and female reproductive tract [32–36]. Here, we postulated that neutrophils were associated with migration of CXCR3⁺ CD4⁺T cells and formation of gastric CD4⁺T_{RM} cells.

In our previous study, an alum-based vaccine caused granulation formation in the stomach [8], and we could not ignore the chronic cognitive dysfunction, toxicity and autoimmunity induced by alum adjuvant [36–38]. In contrast, SF has the advantages of slow release, absorption, and *in situ* gelatinization in various tissues [40,41], SF has been used as a medicinal transmission system [42–44] and as a fixed culture of mesenchymal cells *in vivo* [45]. In this study, SF, as a vaccine carrier, not only reduced stomach damage but also resulted in pronounced infiltration and generation of gastric intraepithelial CD4⁺T_{RM} cells. The gastric inflammatory response and subsequent infiltration of IFN- γ /IL-17A-producing CD4⁺T cells are sufficient to reduce colonization of Hp [46,47]. Hence, we showed that gastric intraepithelial T_{RM} cells could provide optimal protection independently of additional recruitment of T cells from the circulation. And monocytes and neutrophils participated in the early immune protection against *H. felis* insult. Inflammatory monocytes and neutrophils are important mediators of protection against

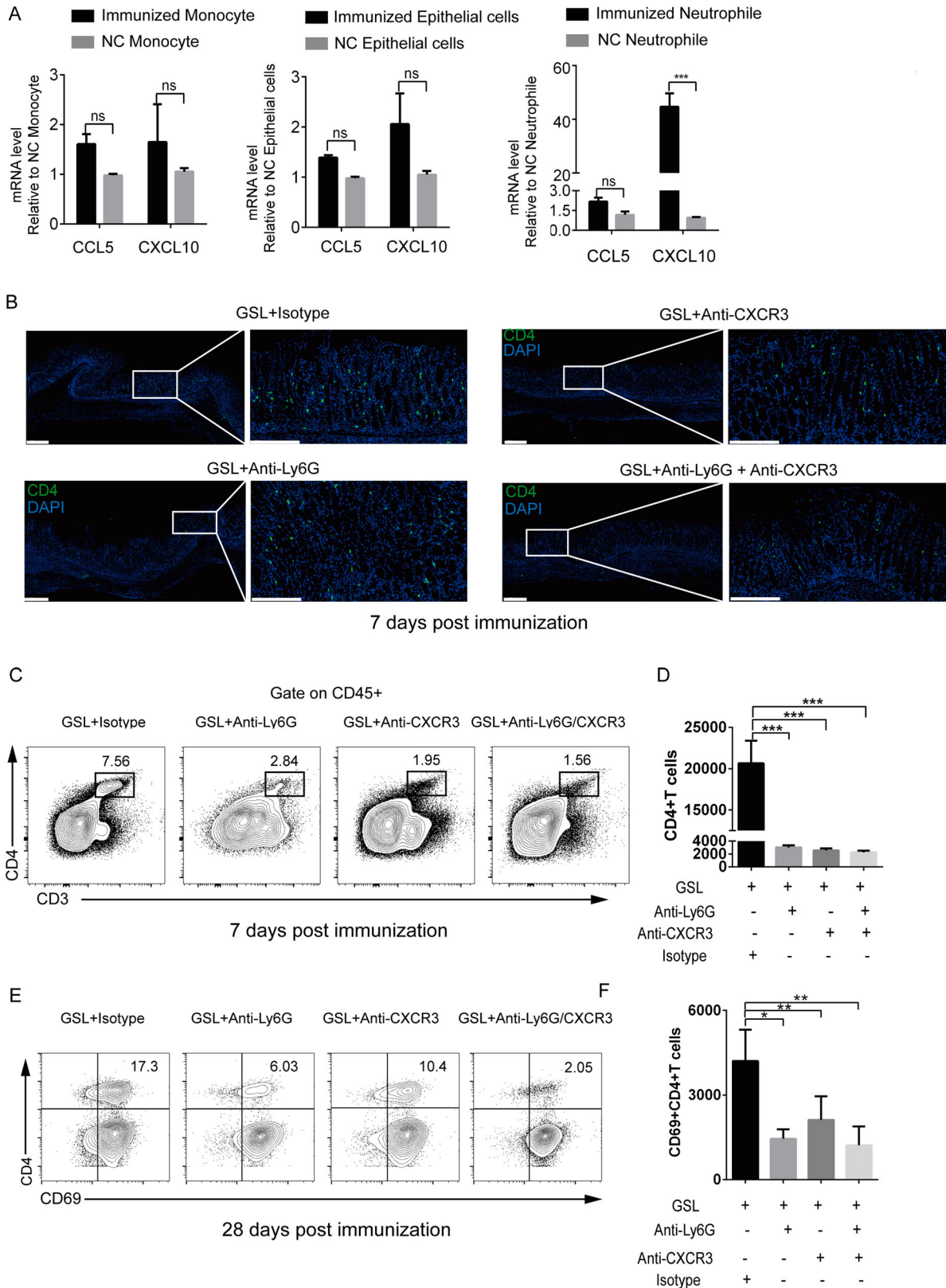


Figure 6. CXCR3 regulated entry into the gastric epithelium and formation of vaccine-induced CD4+TRM cells. (A) Mice were immunized with CCF+SF by GSL vaccination, as described in Figure 1. The stomach was harvested 3 days after immunization, and the number of neutrophils, monocytes and epithelial cells was sorted using a cell sorter for detecting mRNA expression of CXCL10 and CCL5. The neutrophils and monocytes from the blood of naive mice, and epithelial cells from the stomach of naive mice, were the negative control. (B–F) Mice were treated with anti-Ly6G antibody, anti-CXCR3 antibody or isotype (Armenian Hamster IgG and Rat IgG2a) daily. Three days later, mice were immunized with CCF+SF by the GSL, as described in Figure 1. (B) At 7 days after immunization, frozen sections of gastric tissue from immunized mice were stained with antibodies against CD4 (green), and nuclei are depicted by DAPI (blue); scale bar = 100 μ m. (C and D) At 7 days after immunization, the population of CD4+T cells from within the gastric epithelium of mice was analysed using flow cytometry. (E and F) At 28 days after immunization, the population of CD69+CD4+TRM cells from within the gastric epithelium of mice was analysed using flow cytometry. Values are the mean \pm SD ($n = 5$). Data are representative of two independent experiments. P -values were tested using ANOVA. * $P < 0.05$, ** $P < 0.01$, *** $P < 0.001$.

various viral, bacterial, fungal and parasitic infections [47–51]. A recent study demonstrated that CD8 T_{RM} cells trigger protective innate and adaptive immune responses against re-infection by the lymphocytic choriomeningitis virus [3]. Collectively, our data suggest that SF, as a vaccine carrier, optimized a mouse model with pronounced infiltration and distribution of CD4+T_{RM} cells in the gastric epithelium, which conferred optimal protection against *H. felis* insult.

Conclusions

We identified a novel mechanism of local inflammatory response that was involved in the formation of gastric T_{RM} cells. In particular, neutrophils were associated with migration of CD4+T cells into the gastric epithelium and formation of CD4+T_{RM} cells which are critical for protection against *Helicobacter felis*.

We will continue to optimize the vaccination approach, and one of the attractive (yet challenging) options is to design a feasible delivered system that targets the gastric mucosa. For instance, a recent study indicated that oral delivery of insulin targets the gastric mucosa by a self-orienting system [52]. We expect that delivery system is applicable for gastric mucosa-targeted Hp vaccination, and induces formation of gastric intraepithelial CD4+T_{RM} cells against Hp infection.

Acknowledgements

We thank Charlesworth Group (<http://www.charlesworthauthorservices.com>) and Dr. Xu for English language editing. Chupeng Hu carried out statistical analyses, participated in most experiments and drafted the manuscript. Wei Liu, Tao Xi and Yingying Xing conceived the study and participated in its design. Ningyin Xu, An Huang participated in the animal experiments. Zhenxing Zhang, Menghui Fan and Guojing Ruan participated in some animal experiments. All authors read and approved the final manuscript.

Disclosure statement

No potential conflict of interest was reported by the author(s).

Funding

This work was supported by National Natural Science Foundation of China (No. 81971562), National Key Research and Development Project (No. 2017YFD0400303), Postgraduate Research & Practice Innovation Program of Jiangsu Province, The Priority Academic Program Development (PAPD) of Jiangsu Higher Education Institutions, Six Talent Peaks Project in Jiangsu Province (No. 2018-WSW-003).

Availability of data and materials

All data generated or analysed during this study are included in this manuscript and its supplementary information files.

References

- Jiang X, Clark RA, Liu L, et al. Skin infection generates non-migratory memory CD8+ T(RM) cells providing global skin immunity. *Nature*. 2012;483:227–231.
- Teijaro JR, Turner D, Pham Q, et al. Cutting edge: tissue-retentive lung memory CD4 T cells mediate optimal protection to respiratory virus infection. *J Immunol*. 2011;18711:5510–5514.
- Schenkel JM, Fraser KA, Beura LK, et al. T cell memory. resident memory CD8 T cells trigger protective innate and adaptive immune responses. *Science*. 2014;346:98–101.
- Laidlaw BJ, Zhang N, Marshall HD, et al. CD4+ t cell help guides formation of CD103+ lung-resident memory CD8+ T cells during influenza viral infection. *Immunity*. 2014;41:633–645.
- Mackay LK, Stock AT, Ma JZ, et al. Long-lived epithelial immunity by tissue-resident memory T (TRM) cells in the absence of persisting local antigen presentation. *Proc Natl Acad Sci USA*. 2012;109:7037–7042.
- Wakim LM, Woodward-Davis A, Liu R, et al. The molecular signature of tissue resident memory CD8 T cells isolated from the brain. *J Immunol*. 2012;189:3462–3471.
- Carbo A, Olivares-Villagómez D, Hontecillas R, et al. Systems modeling of the role of interleukin-21 in the maintenance of effector CD4+ T cell responses during chronic *Helicobacter pylori* infection. *mBio*. 2014;5:e01243–14.
- Liu W, Zeng Z, Luo S, et al. Gastric subserous vaccination with *Helicobacter pylori* vaccine: an attempt to establish tissue-resident CD4+ memory T cells and induce prolonged protection. *Front Immunol*. 2019;10:1115.
- Mueller SN, Mackay LK. Tissue-resident memory T cells: local specialists in immune defence. *Nat Rev Immunol*. 2016;16:79–89.
- Zaid A, Mackay LK, Rahimpour A, et al. Persistence of skin-resident memory T cells within an epidermal niche. *Proc Natl Acad Sci USA*. 2014;111:5307–5312.
- Iijima N, Iwasaki A. T cell memory. A local macrophage chemokine network sustains protective tissue-resident memory CD4 T cells. *Science*. 2014;346:93–98.
- Shin H, Iwasaki A. A vaccine strategy that protects against genital herpes by establishing local memory T cells. *Nature*. 2012;491:463–467.
- Mackay LK, Rahimpour A, Ma JZ, et al. The developmental pathway for CD103(+)CD8+ tissue-resident memory T cells of skin. *Nat Immunol*. 2013;14:1294–1301.
- Schleimer RP, Kato A, Kern R, et al. Epithelium: at the interface of innate and adaptive immune responses. *J Allergy Clin Immunol*. 2007;120:1279–1284.
- Rimoldi M, Chieppa M, Larghi P, et al. Monocyte-derived dendritic cells activated by bacteria or by bacteria-stimulated epithelial cells are functionally different. *Blood*. 2005;106:2818–2826.
- Rimoldi M, Chieppa M, Salucci V, et al. Intestinal immune homeostasis is regulated by the crosstalk

- between epithelial cells and dendritic cells. *Nat Immunol.* 2005;6:507–514.
- [17] Mueller SN, Zaid A, Carbone FR. Tissue-resident T cells: dynamic players in skin immunity. *Front Immunol.* 2014;5:332.
- [18] Tan Z, Liu W, Liu H, et al. Oral *Helicobacter pylori* vaccine-encapsulated acid-resistant HP55/PLGA nanoparticles promote immune protection. *Eur J Pharm Biopharm: Off J Arbeitsgemeinschaft fur Pharmazeutische Verfahrenstechnik.* 2017;111:33–43.
- [19] Zeng Z, Liu W, Luo S, et al. Shape of gastrointestinal immunity with non-genetically modified *Lactococcus lactis* particles requires commensal bacteria and myeloid cells-derived TGF- β 1. *Appl Microbiol Biotechnol.* 2019;103:3847–3861.
- [20] Dhume K, Finn CM, Strutt TM, et al. T-bet optimizes CD4 T-cell responses against influenza through CXCR3-dependent lung trafficking but not functional programming. *Mucosal Immunol.* 2019;12:1220–1230.
- [21] Myers GA, Ermak TH, Georgakopoulos K, et al. Oral immunization with recombinant *Helicobacter pylori* urease confers long-lasting immunity against *Helicobacter felis* infection. *Vaccine.* 1999;17:1394–1403.
- [22] Michetti P, Corthésy-Theulaz I, Davin C, et al. Immunization of BALB/c mice against *Helicobacter felis* infection with *Helicobacter pylori* urease. *Gastroenterology.* 1994;107:1002–1011.
- [23] Surh CD, Boyman O, Purton JF, et al. Homeostasis of memory T cells. *Immunol Rev.* 2006;211:154–163.
- [24] Sowell RT, Rogozinska M, Nelson CE, et al. Cutting edge: generation of effector cells that localize to mucosal tissues and form resident memory CD8 T cells is controlled by mTOR. *J Immunol.* 2014;193:2067–2071.
- [25] Wein AN, McMaster SR, Takamura S, et al. CXCR6 regulates localization of tissue-resident memory CD8 T cells to the airways. *J Exp Med.* 2019;216:2748–2762.
- [26] Campbell JJ. The chemokine receptor CCR4 in vascular recognition by cutaneous but not intestinal memory T cells. *Nature.* 1999;400:776–780.
- [27] Reiss Y. CC chemokine receptor (CCR)4 and the CCR10 ligand cutaneous T cell-attracting chemokine (CTACK) in lymphocyte trafficking to inflamed skin. *J Exp Med.* 2001;194:1541–1547.
- [28] Lefrançois L, Parker CM, Olson S, et al. The role of (7 integrins in CD8 T cell trafficking during an antiviral immune response. *J Exp Med.* 1999;189:1631–1638.
- [29] Zabel BA, Agace WW, Campbell JJ, et al. Human G protein-coupled receptor Gpr-9-6/Cc chemokine receptor 9 is selectively expressed on intestinal homing T lymphocytes, mucosal lymphocytes, and thymocytes and is required for thymus-expressed chemokine-mediated chemotaxis. *J Exp Med.* 1999;190:1241–1256.
- [30] Slutter B, Pewe LL, Kaech SM, et al. Lung airway-surveillance CXCR3(hi) memory CD8(+) T cells are critical for protection against influenza A virus. *Immunity.* 2013;39:939–948.
- [31] Kohlmeier JE, Reiley WW, Perona-Wright G, et al. Inflammatory chemokine receptors regulate CD8(+) T cell contraction and memory generation following infection. *J Exp Med.* 2011;208:1621–1634.
- [32] Harris TH, Banigan EJ, Christian DA, et al. Generalized Levy walks and the role of chemokines in migration of effector CD8+ T cells. *Nature.* 2012;486:545–548.
- [33] Nakanishi Y, Lu B, Gerard C, et al. CD8(+) t lymphocyte mobilization to virus-infected tissue requires CD4 (+) T-cell help. *Nature.* 2009;462:510–513.
- [34] Schenkel JM, Fraser KA, Vezys V, et al. Sensing and alarm function of resident memory CD8(+) T cells. *Nat Immunol.* 2013;14:509–513.
- [35] Groom JR, Luster AD. CXCR3 ligands: redundant, collaborative and antagonistic functions. *Immunol Cell Biol.* 2011;89:207–215.
- [36] Pineton de Chambrun G, Body-Malapel M, Frey-Wagner I, et al. Aluminum enhances inflammation and decreases mucosal healing in experimental colitis in mice. *Mucosal Immunol.* 2014;7:589–601.
- [37] Couette M, Boisse MF, Maison P, et al. Long-term persistence of vaccine-derived aluminum hydroxide is associated with chronic cognitive dysfunction. *J Inorg Biochem.* 2009;103:1571–1578.
- [38] Tomljenovic L, Shaw CA. Mechanisms of aluminum adjuvant toxicity and autoimmunity in pediatric populations. *Lupus.* 2012;21:223–230.
- [39] Omenetto FG, Kaplan DL. New opportunities for an ancient material. *Science.* 2010;329:528–531.
- [40] Piskin E. Biodegradable polymers as biomaterials. *J Biomater Sci Polym Ed.* 1995;6:775–795.
- [41] Pritchard EM, Kaplan DL. Silk fibroin biomaterials for controlled release drug delivery. *Expert Opin Drug Deliv.* 2011;8:797–811.
- [42] Wenk E, Meinel AJ, Wildy S, et al. Microporous silk fibroin scaffolds embedding PLGA microparticles for controlled growth factor delivery in tissue engineering. *Biomaterials.* 2009;30:2571–2581.
- [43] Guzewicz N, Best A, Perez-Ramirez B, et al. Lyophilized silk fibroin hydrogels for the sustained local delivery of therapeutic monoclonal antibodies. *Biomaterials.* 2011;32:2642–2650.
- [44] Fan H, Liu H, Toh SL, et al. Anterior cruciate ligament regeneration using mesenchymal stem cells and silk scaffold in large animal model. *Biomaterials.* 2009;30:4967–4977.
- [45] Sun H, Yuan H, Tan R, et al. Immunodominant antigens that induce Th1 and Th17 responses protect mice against *Helicobacter pylori* infection. *Oncotarget.* 2018;9:12050–12063.
- [46] Lim JK, Obara CJ, Rivollier A, et al. Chemokine receptor Ccr2 is critical for monocyte accumulation and survival in West Nile virus encephalitis. *J Immunol.* 2011;186:471–478.
- [47] Blanchard TG, Yu F, Hsieh CL, et al. Severe inflammation and reduced bacteria load in murine *helicobacter* infection caused by lack of phagocyte oxidase activity. *J Infect Dis.* 2003;187(10):1609–1615.
- [48] Moyat M, Mack M, Bouzourene H, et al. Role of inflammatory monocytes in vaccine-induced reduction of *Helicobacter felis* infection. *Infect Immun.* 2015;83:4217–4228.
- [49] Osterholzer JJ, Chen GH, Olszewski MA, et al. Accumulation of CD11b+ lung dendritic cells in response to fungal infection results from the CCR2-mediated recruitment and differentiation of Ly-6C high monocytes. *J Immunol.* 2009;183:8044–8053.
- [50] Robben PM, LaRegina M, Kuziel WA, et al. Recruitment of Gr-1+ monocytes is essential for control of acute toxoplasmosis. *J Exp Med.* 2005;201:1761–1769.
- [51] Abramson A, Caffarel-Salvador E, Khang M, et al. An ingestible self-orienting system for oral delivery of macromolecules. *Science.* 2019;363:611–615.